PROPERTIES OF RELATIVISTIC JETS IN EIGHT GAMMA-RAY BURST AFTERGLOWS

A. PANAITESCU
Dept. of Astrophysical Sciences, Princeton University, Princeton, NJ 08544
AND
P. KUMAR
Institute for Advanced Study, Olden Lane, Princeton, NJ 08540

ABSTRACT

We extend our calculation of physical parameters of GRB afterglows through modelling of their broadband emission to three other cases: 980519, 000926, and 010222. Together with 990123, 990510, 991208, 991216, and 000301c, there are eight afterglows whose optical and radio emission allow determination of the burst collimation. The jet energies (after the GRB phase) obtained for this sample of eight afterglows are consistent with a universal value, $\sim 3 \times 10^{50}$ erg, despite a relatively broad distribution of the jet initial half-angle ($2^o - 14^o$).

We find that homogeneous external media are consistent with the emission of all these afterglows while, with a couple of exceptions, wind density profiles are incompatible with the observed multi-wavelength light-curves. The circum-burst densities we found are in the $0.1 - 50$ cm^{-3} range with the exception of 990123 (and 980703), for which this density is below 10^{-2} cm^{-3}. This suggests that, if GRBs are due to collapsars, the wind expelled by the GRB progenitor is rather weak and the circumburst environment is associated with the superbubbles formed by clusters of massive stars.

If for all eight cases the observed GRB durations are close to the ejecta deceleration timescale, then the parameters obtained here lead to jet initial bulk Lorentz factors between 70 and 300 and jet masses around $10^{-6} M_\odot$, implying that the initial baryonic load of the jet is $10^{-5} - 10^{-4}$ of the mass of the GRB progenitor contained within the jet aperture. Our results on the jet energy, opening, Lorentz factor, and evacuation of material until break-out provide constraints on theoretical models of GRB jets.

Subject headings: gamma-rays: bursts - ISM: jets and outflows - methods: numerical - radiation mechanisms: non-thermal - shock waves

1. INTRODUCTION

The localization of Gamma-Ray Bursts (GRBs) to within a few arc-minutes by the Italian–Dutch satellite BeppoSAX, the Interplanetary Network, and the Rossi–X-ray Transient Explorer have enabled us to carry out ground-based follow-up searches for afterglow emission. The current database of multi-wavelength (radio, millimeter, optical, and X-ray) observations allows us to begin a statistical study of the physical properties of GRB afterglows.

This is a third in a series of papers modelling the broadband emission of GRB afterglows, with the aim of determining the total energy in the relativistic ejecta, the jet opening angle, the density and profile of the medium in the immediate vicinity ($\lesssim 10^{18}$ cm) of the burst, and the micro-physical shock parameters. In the first paper (Panaitescu & Kumar 2001) we have modeled four afterglows (980703, 990123, 990510, 991216), while in a second paper (Panaitescu 2001a) we analyzed the peculiar afterglow 000301c, whose emission exhibited a sharp break followed by a steep decay. Here we present our results for the afterglows 980519, 000926, and 010222. The decay of the optical and/or the radio emission of all these bursts, except 980703, steepened after about 1 day, which is usually interpreted as evidence for collimation of ejecta (Rhoads 1999).

In §2 we summarize the principal aspects of our modelling, the unknown parameters, and describe an analytic method for determining afterglow parameters. In §3 we review the properties of the models for individual afterglows. The analysis of the results obtained for eight GRBs and their implications on the nature of the central explosion are presented in §4.

2. THE AFTERGLOW MODEL

The calculation of the afterglow emission is carried out in the standard framework of relativistic ejecta decelerated by an external medium (Mészáros & Rees 1997), with allowance for the effects due to collimation (Rhoads 1999). The equations governing the dynamics of jet–medium interaction and those for the calculation of the synchrotron and inverse Compton emission are detailed by Panaitescu & Kumar (2000, 2001). Similar analytical treatments of jet dynamics and/or emission of radiation can be found in Waxman (1997), Granot, Piran & Sari (1999), Gruzinov & Waxman (1999), Wijers & Galama (1999), Chevalier & Li (2000), Dai & Lu (2000), Kumar & Panaitescu (2000), and Sari & Esin (2001). The effect of interstellar scintillation on the radio afterglow emission (Goodman 1997) is taken into account following the treatment of Walker (1998).

The afterglow modelling has the following basic features:
i) the jet is considered uniform, with an energy per solid angle independent of direction, and with sharp edges;
ii) the shocked gas internal energy density is assumed uniform;
iii) the jet dynamics is calculated by following the evolution of its energy (which decreases due to radiative losses), mass (increasing, as the jet sweeps-up the surrounding medium), and aperture (which increases due to jet expansion in the co-moving frame). The coupled, differential equations for the jet dynamics are given in Kumar & Panaitescu (2000) and Panaitescu & Kumar (2001);
iv) the equations for the jet dynamics and calculation of radiation are accurate in any relativistic regime;
v) the shock-accelerated electron distribution is a power-law

$\mathcal{N}(\gamma) \propto \gamma^{-p}$ in the random electron Lorentz factor γ, starting from a minimum γ_i up to a high energy break γ_*, the latter being relevant if $p \lesssim 2$;
$vi)$ the afterglow emission is calculated by integrating over the jet dynamics the synchrotron and inverse Compton radiation, taking into account the spread in the arrival time of photons emitted at a given radius;
$vii)$ the observer is assumed to lie on the jet axis. Our results for the jet parameters are basically insensitive to offsets less than the jet opening angle (Kumar & Panaitescu 2000).

The model has three parameters that give the jet dynamics: the initial jet energy E_0, initial half-angle θ_0, and external particle density n (or the constant A for a wind-like density profile[1] $n(r) = Ar^{-2}$), and three parameters related to the microphysics of shocks: the fraction ε_B of the post-shock energy density in magnetic fields, the fractional energy ε_e in electrons if they all had the same Lorentz factor γ_i, and the power-law index p. For $p \lesssim 2$ the fractional energy ϵ of the electrons between γ_i and γ_* is used to parameterize γ_*, while for the shape of the cut-off above it we assume, for simplicity, a steeper power-law of index q.

The spectrum of the afterglow synchrotron emission has breaks at the self-absorption frequency ν_a, injection frequency ν_i corresponding to the minimum electron γ_i, cooling frequency ν_c corresponding to the electron Lorentz factor for which the radiative timescale equals the dynamical time, and cut-off frequency ν_* associated with γ_*. Generically, the afterglow emission F_ν can be written as

$$F_\nu = F_p\ \nu_a^{-\beta_a} \nu_i^{-\beta_i} \nu_c^{-\beta_c} \nu_*^{-\beta_*}\ \nu^{\beta_a+\beta_i+\beta_c+\beta_*}\ , \qquad (1)$$

where β_x ($x \equiv a, i, c, *$) is non-zero for break frequencies ν_x between ν and $\nu_p \equiv \min(\nu_c, \nu_i)$, F_p being the flux at ν_p.

As implied by equation (1) the afterglow light-curve at a given frequency is determined by the evolution of the peak flux F_p and spectral break frequencies ν_a, ν_i, ν_c and ν_*. Assuming constant parameters ε_B, ε_e and ϵ, the evolution of these spectral characteristic quantities is determined by that of Γ, the Lorentz factor of the jet, its radius r and by the external density profile $n(r)$. For a highly relativistic jet and negligible radiative losses, conservation of total jet energy leads to $\Gamma \propto t^{-3/8}$ and $r \propto t^{1/4}$ in the case of a homogeneous medium and $\Gamma \propto t^{-1/4}$, $r \propto t^{1/2}$ for a wind external medium, *before* t_j when the jet transits between a quasi-spherical expansion and a lateral spreading dominated one. *After* t_j the jet dynamics is described by $\Gamma \propto t^{-1/2}$ and (to "zeroth order") $r \sim$ constant.

The resulting time behaviours of the afterglow spectral characteristics in these two asymptotic regimes are summarized in Table 1, together with the afterglow light-curve $t^{-\alpha}$ at frequencies above ν_i, assuming $\nu_i < \nu_c$ (slowly cooling electrons) and $\nu_c \ll \nu_*$. The afterglow temporal behaviour depends only on the index p of the electron distribution (or q above γ_*), therefore it can be readily determined from optical or X-ray observations *if* the locations of the break frequencies ν_i, ν_c (and ν_*, if relevant) relative to the observing frequency are known. For measurements made more than a few hours after the GRB, the injection frequency is below the optical domain, thus the only uncertainties are related to ν_c (and ν_*). Consistency between the decay indices $\alpha(p)$ given in Table 1 and the slope $\beta(p)$ of the synchrotron power-law optical spectrum $F_\nu \propto \nu^{-\beta}$, where

$$\beta = \frac{1}{2}\ (p-1) \text{ for } \nu_i < \nu < \nu_c\ , \quad \beta = \frac{1}{2} \text{ for } \nu_c < \nu\ , \quad (2)$$

is commonly used to determine both p and the location of ν_c relative to the optical domain.

Another parameter that can be easily determined, though only roughly, from observations is the jet initial half-aperture, θ_0, provided that the afterglow decay exhibits an achromatic steepening. Such a light-curve break is expected to occur when the jet Lorentz factor decreases to θ^{-1}, which is also roughly the time when the jet lateral expansion becomes significant. This happens around

$$t_j = 0.4\ (z+1)\ \left(E_{0,50} n_0^{-1}\right)^{1/3} \theta_{0,-1}^2 \text{ day}\ , \qquad (3)$$

where the coefficient has been determined numerically, using the arrival time of the photons moving toward the observer along the jet axis, z is the burst redshift, $E_{0,50}$ the initial jet energy measured in 10^{50} erg, n_0 the external medium density in cm^{-3}, and $\theta_{0,-1}$ the initial jet half-opening measured in 0.1 radians. The strong dependence of t_j on θ_0 given in equation (3) can be used to constrain the initial jet aperture from the time when the afterglow light-curve breaks. As we shall see, the external medium density varies among burst by at least three orders of magnitude, thus θ_0 inferred from of equation (3) is uncertain by a factor $\gtrsim 2$.

Thus two basic afterglow parameters, p and θ_0, can be determined from the optical afterglow temporal behaviour, with minimal use of spectral information. Finding the remaining parameters, four if the high frequency cut-off ν_* is above the highest observing frequency, six in the opposite case, is conditioned by the localization of the spectral breaks at some time (not necessarily the same for all breaks), either from the afterglow flux at two frequencies bracketing a given break, or from the passage of that break through an observing band.

As an example, consider a highly relativistic jet undergoing an adiabatic expansion at $t \ll t_j$, when there is little lateral spreading, and let us assume that the electron radiative cooling is synchrotron-dominated. In this case it can be shown that the break frequencies and peak flux are powers in the model parameters:

$$\begin{aligned}
\nu_a &\sim 2\ (z+1)^{-1}\ \mathcal{E}_{0,53}^{1/5}\ n_0^{3/5}\ \varepsilon_{e,-1}^{-1}\ \varepsilon_{B,-2}^{1/5} && \text{GHz} \\
\nu_i &\sim 20\ (z+1)^{1/2}\ t_d^{-3/2}\ \mathcal{E}_{0,53}^{1/2}\ \varepsilon_{e,-1}^{2}\ \varepsilon_{B,-2}^{1/2} && \text{THz} \\
\nu_c &\sim 600\ (z+1)^{-1/2}\ t_d^{-1/2}\ \mathcal{E}_{0,53}^{-1/2}\ n_0^{-1}\ \varepsilon_{B,-2}^{-3/2} && \text{THz} \\
F_p &\sim 20\ (z+1) D_{L,28}^{-2}\ \mathcal{E}_{0,53}\ n_0^{1/2}\ \varepsilon_{B,-2}^{1/2} && \text{mJy}
\end{aligned} \qquad (4)$$

where $\mathcal{E}_{0,53}$ is the isotropic-equivalent initial jet energy in 10^{53} erg,[2] ε_e and ε_B have been normalized to 0.1 and 0.01 respectively, t_d is the observer time measured in days, and $D_{L,28}$ is the burst luminosity distance measured in 10^{28} cm.

Thus if we know ν_a, ν_i, ν_c and F_p from observations, inverting the set of equations (4) above allows the calculation of $\mathcal{E}_0$ (which together with θ_0 gives the jet energy E_0), n, ε_e and ε_B. This method was used for the afterglow of GRB 970508 by Granot et al. (1999) and Wijers & Galama (1999), however it cannot be readily applied to other afterglows, as the locations of

[1] This constant is proportional to the ratio between the mass loss rate of the star which ejects the wind and the speed of this wind. We shall denote by A_* the value of the constant A relative to that corresponding to $10^{-5}\ M_\odot$ ejected per year at a speed of 1000 km/s.

[2] At $t < t_{jet}$, when the jet edge is not yet visible, the afterglow emission is determined by the isotropic equivalent $\mathcal{E}_0$ of the jet energy, rather than E_0.

ν_a and ν_c are not well constrained by the available data.[3] Apart from this limitation, the approximations usually made in analytical treatments of the afterglow emission (e.g. Waxman 1997, Wijers & Galama 1999, Panaitescu & Kumar 2000, Sari & Esin 2001) are accurate only over a limited time interval, numerical calculations being needed to account for various complications, such as:
i) moderately relativistic jets, with Γ of several,
ii) jets transiting between quasi-collimated and lateral-spreading expansion,
iii) electron radiative cooling not dominated by a single emission process (synchrotron or inverse Compton),
iv) afterglow spectral breaks smoothed by the differential relativistic boost and arrival time over the jet surface,
v) time changing ordering of the spectral, during the afterglow evolution,
and to yield a more reliable determination of jet parameters.

3. COLLIMATED AFTERGLOWS

The model outlined above was used to model the broadband emission of eight afterglows – 980519, 990123, 990510, 991208, 991216, 000301c, 000926, and 010222 – to determine the parameters E_0, θ_0, n (or A_* for a wind), ε_e, ε_B, and p (plus ϵ and q, if relevant) by χ^2-minimization, i.e. maximization of the likelihood to obtain the observed fluxes. In calculating the afterglow optical fluxes, we assumed a 5% error in the magnitude-to-flux conversion and Galactic reddening, and we subtracted the reported contributions of the host or contaminating galaxies. X-ray fluxes have been calculated from the reported band fluxes (2–10 keV, usually) and X-ray spectral slopes.

The above listed eight afterglows were selected based on the existence of: i) a break in the optical light-curve, allowing the calculation of the jet initial opening, and ii) sufficient broadband observations to make the modelling meaningful. Some of the results presented elsewhere (990123, 990510, 991216 – Panaitescu & Kumar 2001, 000310c – Panaitescu 2001a, 991208 – Panaitescu 2001b) are reviewed below. We also present results for three other afterglows (980519, 000926, 010222). The best fit parameters obtained for each afterglow, assuming a homogeneous external medium, and their 90% confidence level intervals are given in Table 2.

3.1. *GRB 980519*

The optical emission of this afterglow had a break of magnitude $\Delta\alpha \simeq 0.5$ at $t \sim 1$ day, with a temporal index $\alpha_o = 2.22 \pm 0.04$ (Jaunsen et al. 2001) after the break, close to that measured in X-rays, $\alpha_x = 2.25 \pm 0.04$, at about 1 day (Nicastro et al. 1999). The equality of the two indices is consistent with a jet interpretation. At $t \lesssim 1$ day, the slope of the optical spectrum dereddened for Galactic extinction, $\beta_o = 1.20 \pm 0.25$ (Halpern et al. 1999), is shallower than that measured by Nicastro et al. (1999) at about the same time in X-rays, $\beta_x = 1.72 \pm 0.42$. The difference between the two slopes is close to that expected when ν_c is between optical and X-rays but, given the their large uncertainties, does not provide a compelling proof.

Numerically we find that the radio (Frail et al. 2000a), optical (Vrba et al. 1999, Jaunsen et al. 2001) and X-ray (Nicastro et al. 1999) emission of 980519 can be well accommodated by a spreading jet interacting with a homogeneous medium, and with ν_c between optical and X-rays (Figure 1). A jet model with a wind medium yields a slightly shallower break than observed in the I-band light-curve of this afterglow over a factor 10 in time and provides a poorer fit to the radio data, with $\chi^2 = 73$ for 46 degrees of freedom.

3.2. *GRB 990123*

An increase of the light-curve decay index α by $\Delta\alpha \sim 0.55$ has been observed (Kulkarni et al. 1999a) at few days in the R-band emission of this afterglow, after subtracting the host galaxy. The break was confirmed in the V-band with HST observations (Fruchter et al. 1999). The best fit to the radio (Kulkarni et al. 1999b, Galama et al. 1999), optical (Castro-Tirado et al. 1999, Galama et al. 1999), and X-ray (Costa 1999) data[4] has a very tenuous external medium of $n < 10^{-3}$ cm^{-3} (Table 2). Marginally acceptable fits can be obtained for $n \sim 10^{-2}$ cm^{-3} and higher values are excluded.

3.3. *GRB 990510*

The sharp break seen at about 1 day in this afterglow, across which the light-curve decay index changed by $\Delta\alpha = 1.4 - 1.7$ (Harrison et al. 1999, Stanek et al. 1999), rules out a wind external medium, for which the steepening should be much more gradual (Kumar & Panaitescu 2000). The quasi-flat radio emission seen between 1 and 10 days, when the optical break occurred, is consistent with the analytical expectations for a jet emission at $t > t_j$ and $\nu < \nu_i$. In the best fit to the radio (Harrison et al. 1999), optical (Harrison et al. 1999, Stanek et al. 1999) and X-ray (Kuulkers et al. 2000) emission of this afterglow, the cooling frequency is in the optical domain.

3.4. *GRB 991208*

The radio emission of this afterglow (Galama et al. 2000) exhibited a quasi-flat behavior until ~ 10 days, followed by a decay (Galama et al. 2001) which is much shallower than the $t^{-2.2\pm0.2}$ observed in the optical at 2–7 days (Castro-Tirado et al. 2001). Based on these features it can be shown (Panaitescu 2001b) that, within the simplest afterglow jet model presented in §2, the steepening of the radio emission at 10 days is due to the ν_i-passage, and the jet break (t_j) occurred earlier. Then the shallow radio decay after 10 days requires a hard electron distribution and the steep optical decay implies that the ν_*-break is below the optical domain.

The spectral characteristics (break frequencies and peak flux) of the emission from a jet with the parameters given in Table 2 are consistent with those obtained by Galama et al. (2000) by fitting the spectrum of 991208 at four epochs. The data can be fit equally well ($\chi^2 = 110$ for 97 df) with wind medium of $A_* = 0.65$ and a jet with parameters $E_0 = 3.2 \times 10^{50}$ erg, $\theta_0 = 14^o$, $\varepsilon_e = 0.054$, $\varepsilon_B = 0.021$, and $p \sim 1.4$. These parameters are close to those determined by Li & Chevalier (2001), except θ_0, as their calculations were done in the framework of spherical ejecta.

3.5. *GRB 991216*

The 1–100 days 8.5 GHz emission of this afterglow had a $t^{-0.8}$ average decay (Frail et al. 2000b), shallower than that of the optical emission. The R-band light-curve initially fell-off as

[3] Evidence for self-absorption at radio frequencies exists for 970508, 991208, 000301c and, perhaps, 991216.

[4] This is a larger data set than we used previously (Panaitescu & Kumar 2001).

$t^{-1.2}$ and exhibited a break (Halpern et al. 2000) of magnitude $\Delta\alpha = 0.3 - 0.9$ at few days. The lack of a simultaneous break in the radio emission indicates that the optical steepening does not correspond to the jet break but, more likely, to the passage of a spectral feature. Due to the different radio and early optical decay indices it is not possible to model all the data with a quasi-spherical outflow (i.e. a wide jet). We note that the early radio behaviour is consistent with the flat emission at $\nu < \nu_i$ expected from a spreading jet ($t > t_j$), while the passage of ν_i at several days could explain the radio decay at later times. Thus a jet model with $t_j < 1$ day may accommodate the radio emission of this afterglow. Then the shallow radio decay after 10 days and the early $t^{-1.2}$ optical decay require $p \lesssim 1.5$, while the optical steepening seen at $t \gtrsim 1$ day must be tied to the passage of a spectral break. The radio (Frail et al. 2000b), optical (Garnavich et al. 2000, Halpern et al. 2000) and X-ray data can be fit with a homogeneous medium[5] or an r^{-2} wind. In the latter case the best fit has $\chi^2 = 41$ for 41 df, but yields millimeter fluxes slightly exceeding some observational upper limits.

3.6. *GRB 000301c*

The 8.5 GHz emission of this afterglow had a shallow t^{-1} decay after 30 days. The optical light-curves exhibited a slow $t^{-0.7}$ decay followed by a strong break (Jensen et al. 2001) of magnitude $\Delta\alpha \sim 2$ at few days. The interpretation of this break as the signature of a jet (Berger et al. 2000) cannot explain the the difference in the post-break radio and optical decay indices. Moreover, the break is too sharp to be consistent with the gradual transition expected for jets (Kumar & Panaitescu 2000) and too large to be explained with the $p \lesssim 3$ implied by the post-break optical decay index. The long lived t^{-1} decay of the 8.5 GHz emission points toward a spreading jet and a hard electron distribution ($p \sim 1.5$), which also explains the decay index of the pre-break optical emission. The passage of a spectral feature through the optical range is required by the steepening observed at few days and by the softening of the near infrared–optical spectrum observed at the same time (Rhoads & Fruchter 2001). The best fit we obtain for a homogeneous medium is only marginally acceptable. For a wind-like medium, the best fit has $\chi^2 = 140$ for 96 df, thus it is rather unacceptable.

3.7. *GRB 000926*

The X-ray emission (Piro et al. 2001) of this afterglow provided for the first time evidence (Harrison et al. 2001) that the X-ray emission may be inverse Compton scatterings (Panaitescu & Kumar 2000, Sari & Esin 2001). The proof lies in that the extrapolation of the optical spectrum, after dereddening for the host (intrinsic) extinction, falls below the observed X-ray fluxes.

The optical emission of 000926 exhibited a break of magnitude $\Delta\alpha \sim 0.75$ at few days, with a post-break temporal index $\alpha_o \sim 2.35 \pm 0.05$ (Fynbo et al. 2001, Price et al. 2001). If interpreted as a jet break, it requires that $p \sim \alpha_o$, which would imply (eq. [2]) an optical spectrum significantly harder than observed at $t \sim 1$ day: $\beta_o = 1.42 \pm 0.06$ (Fynbo et al. 2001) or $\beta_o = 1.53 \pm 0.07$ (Price et al. 2001). Within the fireball model, consistency between the optical spectral slope and temporal index requires a significant host extinction. From the curvature of the near infrared–optical spectrum, Fynbo et al. (2001) infer $A_V = 0.18 \pm 0.06$, corresponding to an extinction in the observer I-band of 0.4 ± 0.1 magnitudes, thus the dereddened afterglow spectrum has an optical slope $\beta \sim 1$. Then equation (2) and $p \sim 2.35$ imply that ν_c is below the optical domain.

For a homogeneous medium, the best fit obtained with a model with the above features (Figure 2) has a rather large χ^2 (Table 2) and parameters that are close to those obtained Harrison et al. (2001), except E_0 and ε_B, for which we find values 3 times smaller and 8 times larger, respectively. The best fit model with a wind medium has $\chi^2 = 270$ for 102 df, yielding radio fluxes larger than observed, and parameters $E_0 = 2.7 \times 10^{51}$ erg, $\theta_0 = 2.0^{\rm o}$, $A_* = 2.0$, $\varepsilon_e = 0.042$, $\varepsilon_B = 1.6 \times 10^{-4}$, and $p = 2.70$. Note, however, that Harrison et al. (2001) found a significantly better fit ($\chi^2 = 167$ for 114 data points) for a wind medium.

3.8. *GRB 010222*

At $t \sim 0.5$ day the temporal index of optical emission of this afterglow steepened by $\Delta\alpha = 0.6 \pm 0.1$, to a power-law decay of index $\alpha_o = 1.30 - 1.55$ (Masetti et al. 2001), consistent with that of the X-ray emission, $\alpha_x = 1.33 \pm 0.04$, after 0.5 day ('t Zand et al. 2001). The jet interpretation of this break requires a hard electron distribution ($p \sim 1.4$). As in the case of 000926, such a low index p implies (eq. [2]) an optical spectrum harder than observed, $\beta_o = 0.89 \pm 0.03$ (Jha et al. 2001), indicating the existence of significant intrinsic extinction.

Assuming an SMC-like reddening curve, the best fit to the radio (Berger & Frail 2001), optical (Cowsik et al. 2001, Masetti et al. 2001, Sagar et al. 2001, Stanek et al. 2001) and X-ray ('t Zand et al. 2001) data has $A_V = 0.18$ (Figure 3). The anomalously small value ($\lesssim 10^{-3.5}$) obtained for the parameter ε_e for the minimum injected electron Lorentz factor is due to the hardness of the electron distribution. Larger values of ε_e would lower the break frequency ν_* below the X-ray domain, rendering the model incompatible with the X-ray observations. Given the lack of reported radio data for this afterglow, ε_e is not directly constrained by observing the passage of the ν_i frequency through this domain, hence its value is rather uncertain.

For a wind medium, the best fit is poorer, with $\chi^2 = 130$ for 82 df, and parameters $E_0 = 1.7 \times 10^{50}$ erg, $\theta_0 = 2.7^{\rm o}$, $A_* = 0.22$, $\varepsilon_e = 2.1 \times 10^{-4}$, $\varepsilon_B = 1.7 \times 10^{-3}$, and $p = 1.37$.

3.9. *Collimation versus Passage of Spectral Breaks*

The most important feature of an afterglow jet break, occurring at t_j (eq. [3]) when the jet edge becomes visible, is its *achromaticity* over widely separated frequency domains. For five afterglows (980519, 990123, 990510, 000926, 010222), the observed optical steepening can be attributed to the jet break based on the consistency between the general behaviour of the radio emission, the temporal indices of the pre- and post- break optical decays, and the slope of the optical spectrum. However, due to the scarcity of radio and X-ray data or the lack of a sufficiently wide temporal coverage in X-rays around the time of the optical break, the existence of this break at other frequency cannot be proven convincingly.

For three afterglows (991208, 991216, 000301c), the behaviour of the radio emission indicates that t_j is before the time when the optical break was seen and that the electron index is $p \sim 1.5$. On energetic grounds, such an electron distribution must steepen at an electron energy for which the characteristic synchrotron frequency ν_* may be sufficiently low to cross

[5]The χ^2 given in Table 2 is larger than reported by Panaitescu & Kumar (2001), as we reduced the assumed uncertainty in the Galactic extinction from 10% to 5%. Parameter ranges are very similar.

the optical domain at only few days, yielding a *chromatic* light-curve break. The passage of the other two spectral breaks, ν_i and ν_c, through the observing band could also produce a chromatic steepening. As shown by equation (4), ν_i crosses the optical domain within the first few hours, thus it is unlikely that it could explain even the earliest observed optical break, that seen in 010222, which occurred at ~ 0.5 day (this possibility was tested numerically, with negative results). The temporal indices $\alpha = -\mathrm{d}\ln F_\nu/\mathrm{d}\ln t$ given in Table 1 show that magnitude $\Delta\alpha$ of the break caused by the ν_c passage is at most 1/4 for a homogeneous medium and 5/4 for a wind. Thus the $\Delta\alpha$ observed in 980519, 990123, 991216, 000926, and 010222, ranging from 0.3 to 0.9, require a wind medium and electron cooling dominated by inverse Compton scatterings. A simple analytical investigation shows that for all the above afterglows the index p implied by $\Delta\alpha$ leads to pre- and post-break optical spectral slopes (eq. [4]) and temporal indices (Table 1) that are not fully consistent with the observations. Although none of the afterglow optical breaks modeled in this work may be explained by the passage of ν_i or ν_c, such chromatic breaks may be observed in future afterglows.

4. JET PROPERTIES

4.1. *Jet Energy and GRB Efficiency*

The most prominent feature of the fit parameters presented in Table 2 is that the jet energies at the beginning of the afterglow phase span a relatively narrow range, varying between 10^{50} and 4×10^{50} erg. To this eight afterglows we can add 970508, for which Frail, Waxman & Kulkarni (2000) derive a jet energy $\sim 5\times10^{50}$ erg from its long-lived radio emission. We note that, due to radiative losses, at 1 day, the kinetic energies of the jets with the best fit parameters given in Table 1 are between 0.4×10^{50} erg and 3×10^{50} erg, having thus a wider distribution than E_0.

From equation (3), Frail et al. (2001) have calculated θ_0 for various afterglows and found that the energies released during the γ-ray phase are also well clustered, within a decade around 5×10^{50} erg. In Table 3 we list the energy E_γ lost by the jet during the γ-ray phase, calculated from the observed 25 keV–1 MeV GRB fluences and jet apertures in Table 2. For our sample of eight afterglows, we find that E_γ spans more than an order of magnitude, being significantly broader than the distribution of E_0, the jet kinetic energy after the GRB phase.

Table 3 also shows and the implied efficiency $\epsilon_\gamma = E_\gamma/(E_\gamma+E_0)$ of the γ-ray mechanism. We note that, with the exception of 980519, the resulting GRB efficiencies are in the 50%–90% range, most likely exceeding the limits of internal shocks in channeling the dissipated energy into the 25 keV–1 MeV band. This suggests that, during the GRB phase, jets have inhomogeneities on an angular scale smaller than Γ^{-1} (Kumar & Piran 2000).

4.2. *Jet Aperture*

As shown in Table 2, the initial jet aperture varies from 2° to 14°. At 1 day, due to the lateral spreading, the jet angles span the $3^\circ-17^\circ$ interval, having a dynamical range slightly smaller than θ_0, as the narrower jet have undergone more sideways expansion that the wider ones. Given that optical observations are usually made with less than two decades in time, the dependence on the jet break time t_j on θ_0 (eq. [3]) suggests that the true distribution of θ_0 may be even broader. Therefore the mechanism that produces relativistic GRB jets constrains better the energy of the outflow than its collimation.

In Figure 4 we plot E_0, the jet energy after the GRB phase, versus its aperture θ_0. The linear correlation coefficient of these two quantities is $r(E_0,\theta_0) = 0.25\pm0.33$. For the total jet energy and opening angle, $r(E_0+E_\gamma,\theta_0) = 0.45\pm0.07$. Given that we have only 8 cases, neither of these values are very significant statistically, nevertheless they suggest that wider jets are more energetic.

4.3. *External Medium*

Our results show that models with a homogeneous medium can accommodate the broadband emission of all eight afterglows. With the exception of 991208 and 991216, a wind-like external medium provides a poorer fit to the data in all other cases. If our assumptions regarding the jet uniformity is accurate, then a GRB model involving a massive star is allowed in these six cases only if there is a mechanism for homogenizing the wind surrounding the star prior to the its interaction with the jet. Ramirez-Ruiz et al. (2001) have shown that the interaction between the wind of a Wolf-Rayet star and a circumstellar medium of $n = 1\ \mathrm{cm}^{-3}$ leads to the formation of a quasi-uniform, hot shell, of density $\sim 10^3\ \mathrm{cm}^{-3}$, extending from $\gtrsim 10^{16}$ cm up to $\sim 10^{18}$ cm. More tenuous (or colder) media could produce thicker and less dense shells, consistent with the range of densities found here.

The particle density given in Table 2 for homogeneous media range from values typical for the interstellar medium (980519, 990510) to those of diffuse interstellar hydrogen clouds (991208, 991216, 000301c, 000926, 010222). In one case (990123) we find an external density below $10^{-2}\ \mathrm{cm}^{-3}$, characteristic of a hot component of the interstellar medium or a galactic halo. A similar low density was also obtained for the afterglow 980703 (Panaitescu & Kumar 2001). These values are 2–5 orders of magnitude smaller than those implied by the N_H column densities inferred by Galama & Wijers (2001) from the soft X-ray absorption of 980703, 990123, 990510, and 980519. This suggests that either the GRB is not embedded in the absorbing medium or that the gas in the vicinity of the GRB was evacuated.

If GRBs are related with the death of massive stars, as in the collapsar model (Woosley 1993, Paczyński 1998, MacFadyen & Woosley 1999), one would expect higher external densities than inferred by us for this sample of 8 afterglows. Recently, Scalo & Wheeler (2001) have pointed out that the supernovae and winds occurring in a cluster of massive stars form superbubbles within giant molecular clouds, with local densities that could range over few orders of magnitude, possibly being as low as $10^{-3}\ \mathrm{cm}^{-3}$, depending on the superbubble age, ambient medium, power input, and evaporation of clouds and of the shell swept-up by the cluster wind.

4.4. *Jet Mass and Lorentz Factor*

The afterglow emission is only weakly dependent on the initial jet Lorentz factor Γ_0, which determines the evolution of the radiative losses in the early afterglow. Thus Γ_0 cannot be significantly constrained through afterglow modelling. However, the fit jet parameters can be used to determine its jet Lorentz factor Γ at any time during the afterglow phase:

$$\Gamma \simeq 6.3\ (\mathcal{E}_{0,53}/n_0)^{1/8}\ [t/(1+z)]^{-3/8}\ , \qquad (5)$$

with t measured in seconds. Thus Γ_0 could be calculated if the deceleration timescale t_0 were known.

In a few bursts (Giblin et al. 1999, Tkachenko et al. 2000), soft X-ray emission has been observed from the end of the GRB phase up to 10^4 s, indicating that the external shock had already set in by the end of the GRB (at t_γ). In other cases (Pian et al. 2001, 't Zand et al. 2001) there is no detectable X-ray emission after the GRB, suggesting that $t_\gamma < t_0$. In order to constrain Γ_0, we will assume that the observed GRB duration is a good measure of t_0. Equation (5), shows that Γ has a moderate dependence on t, thus the error due to this assumption is likely not too large.

The initial jet Lorentz factor Γ_0 (Table 3) calculated for the best fit parameters (Table 2) are between 70 and 300. From the jet energy E_0 at the beginning of the afterglow phase, one can also calculate the jet mass $M_{jet} = c^{-2}E_0/\Gamma_0$. The resulting values (Table 3), spanning less than a decade around $10^{-6}M_\odot$, are shown against the jet opening in Figure 4. The linear correlation coefficient of M_{jet} and θ_0 is $r(M_{jet}, \theta_0) = 0.56 \pm 0.28$, indicating that wider jets have a larger baryon load. This is what one would expect in the collapsar model, as the jet propagates through the outer part of a massive star. Note that M_{jet} increases slower than θ_0^2, thus the ratio ψ between the jet mass and the stellar mass within the jet opening decreases with increasing θ_0. For a $10\,M_\odot$ star, this ratio is between 10^{-5} and 10^{-4} (Table 3), indicating a highly efficient evacuation of the star along the direction of the jet.

4.5. *Microphysical Parameters*

The results of Table 2 show that the magnetic field is not always close to the equipartition and that the index p of the power-law distribution of shock-accelerated electrons is not universal. In four of the afterglows analyzed here, the shallow fall-off of either the radio or the optical light-curve after the jet break requires $p \sim 1.5$. As shown by Mészáros, Rees & Wijers (1998), the variation of the energy per solid angle within the jet opening leads to light-curve decay indices that depend not only on p. However, after the jet break time t_j, the observer receives radiation from the entire jet surface, so that that the internal structure of the jet should not affect significantly the post jet-break light-curve decay index.

We note that for the afterglows of 991208, 991216, and 000301c, a fractional energy ϵ of the electrons up to γ_* in the 1/3–2/3 range (i.e. close to the equipartition value) implies that the ν_*-break passes through the optical band at few days, providing a natural explanation for the break seen in the optical emission of these afterglows.

5. CONCLUSIONS

Our modelling of the broadband emission of eight afterglows, for which the initial jet opening can be determined sufficiently accurate, reveals several properties of GRB jets, which represent constraints on the models for GRB progenitors (Woosley 1993, Paczyński 1998, Vietri & Stella 1998, MacFadyen & Woosley 1999, Mészáros, Rees & Wijers 1999, MacFadyen, Woosley & Heger 2001):
$i)$ the jet energy is rather well constrained. The values determined here are within a factor of 4, being consistent with a universal value of $\sim 2.5 \times 10^{50}$ erg,
$ii)$ the jet initial aperture spans at least the $2^\circ - 15^\circ$ interval, wider jets being more energetic,
$iii)$ the jet initial Lorentz factor exceeds 100,
$iv)$ if the jet ejection involves its penetration through a stellar envelope, the baryonic mass entrained by the jet is less than 10^{-4} of the material encountered by the jet,
$v)$ the surrounding medium does not have the r^{-2} profile expected for a wind. The density of the external medium ranges from values typical for a galactic halo to those characteristic of diffuse clouds.

The conclusions and the jet parameters presented here were obtained from modelling the afterglow data within a specific framework and under certain assumptions, the most notable being the uniformity of the jet, the isotropy of the external medium, and the constancy of the energy release parameters (ε_e, ε_B). We have attempted to accommodate the emission features of each afterglow with the simplest model possible, requiring a single emission component (synchrotron) and a single power-law electron distribution. For 991208, 991216, and 000301c the latter condition had to be relaxed and a steepening of the electron distribution above a certain energy has been introduced to allow consistency between the shallowness of the radio decay and the steepness of the optical fall-off. For 000926, the former condition has been "abolished" and inverse Compton emission has been used to accommodate the bright X-ray fluxes. Such departures from the standard afterglow model are natural if the injected electron distribution is hard or if the external medium is dense and magnetic field strong. Given that we have used a model with minimal complexity, it is quite conceivable that more sophisticated afterglow models, with more "degrees of freedom" (e.g. structured jet, inhomogeneous external medium) could yield different afterglow parameters and constraints on GRB progenitors.

AP acknowledges the supported received from Princeton University through the Lyman Spitzer, Jr. fellowship.

REFERENCES

Berger, E. et al. 2000, ApJ, 545, 56
Berger, E. & Frail, D. 2001, GCN #968
Castro-Tirado, A. et al. 1999, Science, 283, 2069
Castro-Tirado, A. et al. 2001, A&A, 370, 398
Chevalier, R. & Li, Z. 2000, ApJ, 536, 195
Costa, E. 1999, A&AS 138, 425
Cowsik, R. et al. 2001, BASI, in press (astro-ph/0104363)
Dai, Z. & Lu, T. 2000, ApJ, 537, 803
Frail, D. et al. 2000a, ApJ, 534, 559
Frail, D., Waxman, E. & Kulkarni, S. 2000, ApJ, 537, 191
Frail, D. et al. 2000b, ApJ, 538, L129
Frail, D. et al. 2001, ApJL, submitted (astro-ph/0102282)
Fruchter, A. et al. 1999, ApJ, 519, L13
Fynbo, J. et al. 2001, A&A, 373, 796
Galama, T. et al. 1999, Nature, 398, 394
Galama, T. et al. 2000, ApJ, 541, L45
Galama, T. & Wijers, R. 2001, ApJ, 549, L209
Galama, T. et al. 2001, in preparation
Garnavich, P. et al. 2000, ApJ, 543, 61
Giblin, T. et al. 1999, ApJ, 524, L47
Goodman, J. 1997, New Astronomy, 2, 449
Granot, J., Piran, T. & Sari, R. 1999, ApJ, 527, 236
Gruzinov, A. & Waxman, E. 1999, ApJ, 511, 852
Halpern, J., Kemp, J., Piran, T. & Bershady, M. 1999, ApJ, 517, L105
Halpern, J. et al. 2000, ApJ, 543, 697
Harrison, A. et al. 1999, ApJ, 523, L121
Harrison, A. et al. 2001, ApJ, in press (astro-ph/0103377)
Jaunsen, A. et al. 2001, ApJ, 546, 127
Jensen, B. et al. 2001, A&A, 370, 909
Jha, S. et al. 2001, ApJ, 554, L155
Kulkarni, S. et al. 1999a, Nature, 398, 389
Kulkarni, S. et al. 1999b, ApJ, 522, L97
Kumar, P. & Panaitescu, A. 2000, ApJ, 541, L9
Kumar, P. & Piran, T. 2000, ApJ, 535, 152

Kuulkers, E. et al. 2000, ApJ, 538, 638
Li, Z. & Chevalier R. 2001, ApJ, 551, 940
MacFadyen, A. & Woosley, S. 1999, ApJ, 524, 262
MacFadyen, A., Woosley, S. & Heger, A. 2001, ApJ, 550, 410
Masetti, N. et al. 2001, A&A, 374, 382
Mészáros, P. & Rees, M.J. 1997, ApJ, 476, 232
Mészáros, P., Rees, M.J. & Wijers, R. 1998, ApJ, 499, 301
Mészáros, P., Rees, M.J. & Wijers, R. 1999, New Astronomy, 4, 303
Nicastro, L. et al. 1999, A&A, 138, S437
Paczyński, B. 1998, ApJ, 494, L45
Panaitescu, A. & Kumar, P. 2000, ApJ, 543, 66
Panaitescu, A. & Kumar, P. 2001, ApJ, 554, 667
Panaitescu, A. 2001a, ApJ, 556, 1002
Panaitescu, A. 2001b, ApJ, to be submitted
Pian, E. et al. 2001, A&A, 372, 456
Piro, L. et al. 2001, ApJ, accepted (astro-ph/0103306)
Price, P. et al. 2001, ApJ, 549, L7
Ramirez-Ruiz, E., Dray, L., Madau, P. & Tout, C. 2001, MNRAS, submitted (astro-ph/0012396)
Rhoads, J. 1999, ApJ, 525, 737
Rhoads, J. & Fruchter, A. 2001, ApJ, 546, 117
Sagar, R. et al. 2001, BASI, 29, 91
Sari, R. & Esin, A. 2001, ApJ, 548, 787
Scalo, J. & Wheeler, J.C. 2001, ApJ, submitted (astro-ph/0105369)
Stanek, K., Garnavich, P., Kaluzny, J., Pych, W., & Thompson, I. 1999, ApJ, 522, L39
Stanek, K. et al. 2001, ApJ, in press (astro-ph/0104329)
Tkachenko, A. et al. 2000, A&A, 358, L41
Vietri, M. & Stella, L. 1998, ApJ, 507, L45
Vrba, F. et al. 1999, ApJ, 528, 254
Walker, M. 1998, MNRAS, 294, 307
Waxman, E. 1997, ApJ, 485, L5
Wijers, R. & Galama, T. 1999, ApJ, 523, 177
Woosley, S. 1993, ApJ, 405, 273
't Zand, J. et al. 2001, ApJ, in press (astro-ph/0104362)

TABLE 1. Temporal scaling of spectral parameters and index power-law light-curves at $\nu > \nu_i$, for homogeneous and wind ($n \propto r^{-2}$) media, before and after the jet break time t_j, for synchrotron- ($Y < 1$) or inverse Compton-dominated ($Y > 1$) electron cooling. p is the index of the power-law distribution of injected electrons.

$n \propto$	t/t_j	$\nu_a \propto$	$\nu_i \propto$	$\nu_c \propto$		$F_p \propto$	$-\mathrm{d}\ln F_\nu/\mathrm{d}\ln t$		
							$\nu_i < \nu < \nu_c$	$\nu_c < \nu$	
				$Y < 1$	$Y > 1$			$Y < 1$	$Y > 1$
r^0	< 1	t^0	$t^{-3/2}$	$t^{-1/2}$	$t^{(3p-8)/(8-2p)}$	t^0	$\frac{3}{4}p - \frac{3}{4}$	$\frac{3}{4}p - \frac{1}{2}$	$\frac{3}{4}p - \frac{1}{4-p}$
r^{-2}	< 1	$t^{-3/5}$	$t^{-3/2}$	$t^{1/2}$	$t^{(3p-4)/(8-2p)}$	$t^{-1/2}$	$\frac{3}{4}p - \frac{1}{4}$	$\frac{3}{4}p - \frac{1}{2}$	$\frac{3}{4}p - \frac{p}{8-2p}$
r^0, r^{-2}	> 1	$t^{-1/5}$	t^{-2}	t^0	$t^{(2p-4)/(4-p)}$	t^{-p}	p	p	$p - \frac{p-2}{4-p}$

TABLE 2. Best fit parameters for a homogeneous medium and 90% confidence levels for eight GRB afterglows.

GRB	E_0 (10^{50} erg)	θ_0 (deg)	n (cm^{-3})	ε_e (10^{-2})	ε_B	p	χ^2/df	$n \propto r^{-2}$?
980519[a]	$4.1^{+4.8}_{-1.4}$	$2.3^{+0.2}_{-0.2}$	$0.14^{+0.32}_{-0.03}$	11^{+4}_{-3}	$(3.5^{+32}_{-2.3})\,10^{-5}$	$2.78^{+0.07}_{-0.04}$	53/46	no
990123	$1.5^{+3.3}_{-0.4}$	$2.1^{+0.1}_{-0.9}$	$(1.9^{+0.5}_{-1.5})\,10^{-3}$	13^{+1}_{-4}	$(7.4^{+23}_{-5.9})\,10^{-4}$	$2.28^{+0.05}_{-0.03}$	55/56	no
990510	$1.4^{+4.9}_{-0.5}$	$3.1^{+0.1}_{-0.5}$	$0.29^{+0.11}_{-0.15}$	$2.5^{+3.1}_{-0.6}$	$(5.2^{+42}_{-4.7})\,10^{-3}$	$1.83^{+0.18}_{-0.01}$	36/69	no
991208	$2.4^{+2.8}_{-0.8}$	$12.8^{+1.5}_{-2.2}$	18^{+22}_{-6}	$5.6^{+2.1}_{-0.9}$	$(3.5^{+6.0}_{-2.1})\,10^{-2}$	$1.53^{+0.03}_{-0.03}$	112/97	yes
991216	$1.1^{+1.0}_{-0.4}$	$2.7^{+0.4}_{-1.0}$	$4.7^{+6.8}_{-1.8}$	$1.4^{+0.4}_{-0.3}$	$(1.8^{+3.4}_{-0.7})\,10^{-2}$	$1.36^{+0.03}_{-0.03}$	42/41	yes
000301c	$3.3^{+0.3}_{-0.5}$	$13.7^{+0.6}_{-0.5}$	27^{+5}_{-5}	$6.2^{+1.4}_{-1.3}$	$(7.2^{+3.1}_{-1.5})\,10^{-2}$	$1.43^{+0.05}_{-0.07}$	119/96	maybe
000926	$3.2^{+0.3}_{-0.3}$	$8.1^{+0.5}_{-0.6}$	22^{+5}_{-5}	10^{+2}_{-2}	$(6.5^{+1.5}_{-1.1})\,10^{-2}$	$2.40^{+0.01}_{-0.02}$	159/102	no
010222	$4.0^{+7.3}_{-1.3}$	$4.0^{+0.6}_{-0.4}$	$3.2^{+4.0}_{-0.6}$	$0.02^{+0.01}_{-0.01}$	$(2.0^{+21}_{-1.5})\,10^{-4}$	$1.38^{+0.01}_{-0.01}$	104/82	maybe

[a] redshift unknown. $z = 1$ was assumed.

TABLE 3. Burst properties and jet characteristics inferred from the best fit parameters given in Table 2.

GRB	z	ϕ_γ^a (10^{-5})	E_γ^b (10^{50} erg)	ϵ_γ^c	t_γ^d (s)	Γ_0^e	$\Gamma_0\theta_0$	M_{jet}^f ($10^{-6}M_\odot$)	ψ^g (10^{-5})
980519	1^h	2.5	0.52	0.11	40	250	10	0.90	23
990123	1.60	51	12	0.91	100	300	11	0.28	8.3
990510	1.62	2.6	1.2	0.47	100	140	7.8	0.53	7.2
991208	0.71	10	16	0.87	60	68	15	2.0	1.6
991216	1.02	26	3.8	0.76	30	150	7.0	0.43	7.5
000301c	2.03	0.4	6.3	0.65	10	160	38	1.2	0.82
000926	2.07	2.2	30	0.90	25	130	19	1.4	2.7
010222	1.48	9.2	6.0	0.61	120	110	7.3	2.1	17

[a] observed fluence in the 25 keV–1 MeV range, measured in $\mathrm{erg\ cm^{-2}}$
[b] jet γ-ray energy release
[c] efficiency of γ-ray emission
[d] duration of GRB
[e] jet Lorentz factor at end of GRB
[f] jet mass
[g] evacuation fraction within the jet opening, assuming a $10\,M_\odot$ GRB progenitor
[h] redshift $z = 1$ was assumed

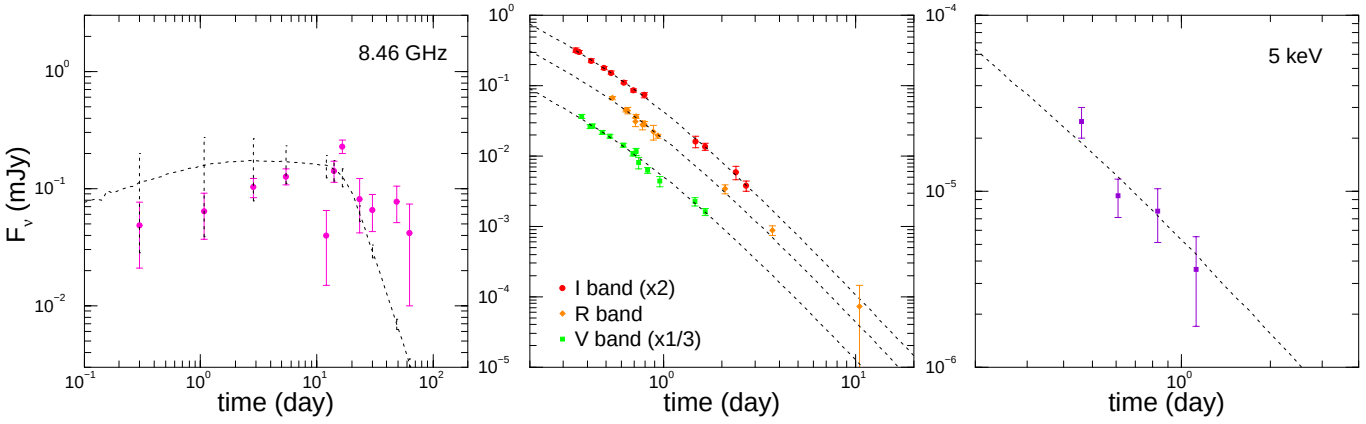

FIG. 1.— Best fit for the afterglow of GRB 980519. The model, whose parameters are given in Table 2, consists of a spreading jet interacting with a homogeneous medium, and cooling frequency between the optical and X-ray domains. Optical data has been corrected for Galactic extinction of $E(B-V) = 0.267$ (Jaunsen et al. 2001). Dotted vertical lines indicate the amplitude of the interstellar scintillation. The I and V band fluxes have been multiplied, for clarity, by the factors indicated. For this afterglow a redshift has not been reported. We have assumed $z = 1$, a value typical for other GRBs.

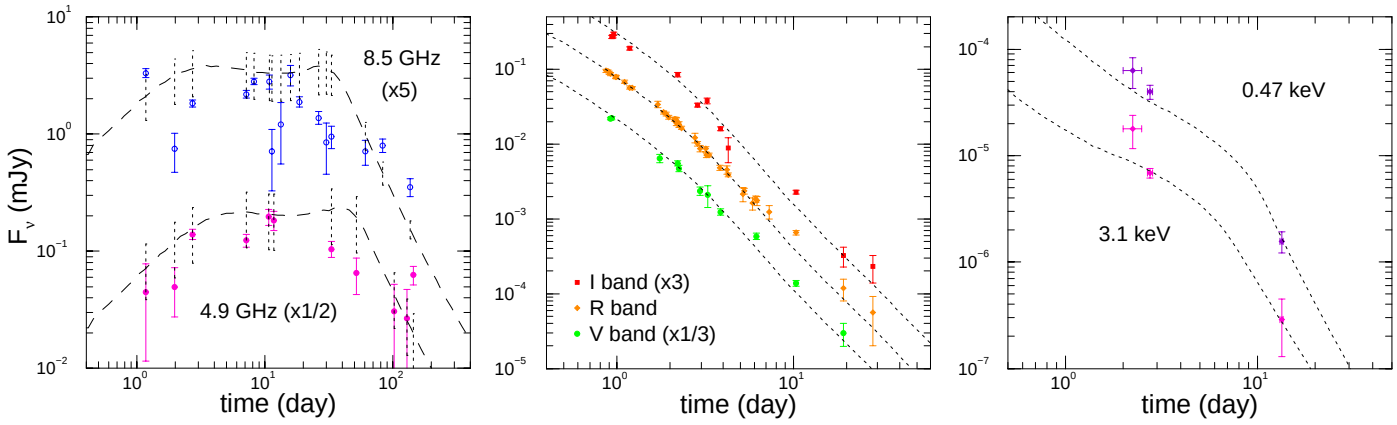

FIG. 2.— Best fit for the afterglow of GRB 000926. The parameters of the jet are listed in Table 2. The cooling frequency lies below the optical domain. Optical measurements have been dereddened for host extinction, assuming an SMC-like reddening curve and $A_V = 0.18$ (Fynbo et al. 2001), and have been corrected for the contamination of $I = 24.50 \pm 0.11$, $R = 25.19 \pm 0.17$, and $V = 26.09 \pm 0.16$ (Price et al. 2001) from a nearby galaxy. The model X-ray emission is due to inverse Compton scatterings, with a significant contribution from synchrotron.

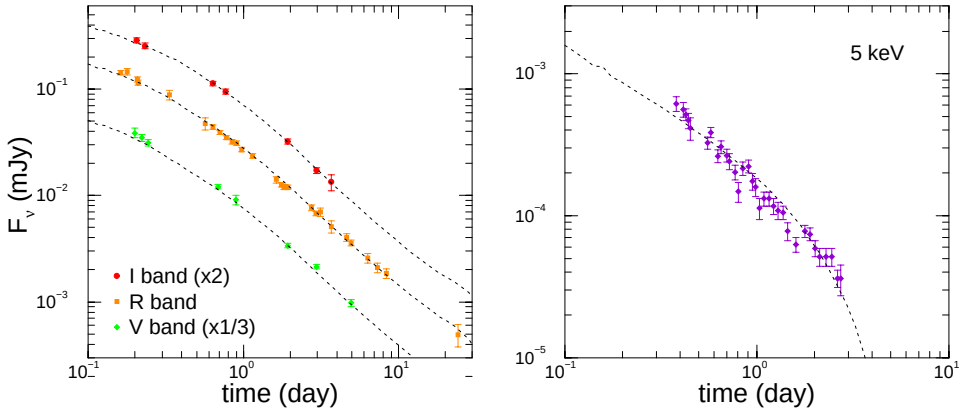

FIG. 3.— Optical and X-ray emission of the afterglow of GRB 010222, and best fit obtained with the parameters given in Table 2. Consistency between the model power-law optical spectrum and the U, B, V, R, I and J measurements available for this afterglow (not all shown in here) implies significant intrinsic reddening. Assuming an SMC-like extinction curve, the best fit to the data is obtained for $A_V = 0.18$ (in the host frame). The model shown here is for a homogeneous medium, and has the cooling frequency slightly below the optical domain.

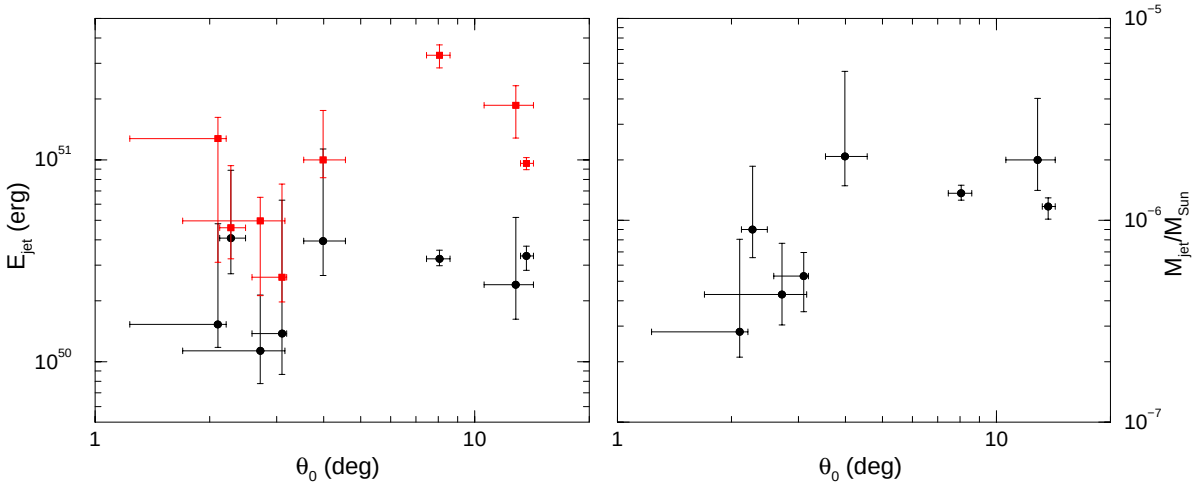

FIG. 4.— Jet energy and mass versus opening angle. Black circles indicate the jet kinetic energies E_0 after the GRB phase, obtained from afterglow modelling. Red squares are for the total jet energy obtained by adding to E_0 the energy $E_\gamma = \mathcal{E}_\gamma \theta_0^2/2$ radiated by the jet during the GRB phase, where $\mathcal{E}_\gamma$ is the isotropic γ-ray energy release. The latter is obtained from the burst redshift and its 25 keV–1 MeV fluence. The jet mass is $M_{jet} = c^{-2} E_0/\Gamma_0$, where Γ_0 (Table 3) is the jet Lorentz factor the ejecta at the end of the GRB (§4.4).